GEOPHYSICAL RESEARCH LETTERS, VOL. 25, NO.15, PAGES 3039-3042, AUGUST 1, 1998

Simulation of the March 9, 1995, substorm: Auroral brightening and the onset of lobe reconnection

J. G. Lyon

Department of Physics, Dartmouth College, Hannover, New Hampshire

R. E. Lopez , C. C. Goodrich

Department of Astronomy, University of Maryland, College Park,

M. Wiltberger, K. Papadopoulos

Department of Physics, University of Maryland, College Park,

Abstract. A global MHD simulation of an isolated substorm that occurred on March 9, 1995 is presented. The simulation, driven with solar wind data provided by the Wind satellite, reproduced to a surprising degree the evolution of substorm activity. The onset of the expansion phase was coincident with the penetration of an electric field spike into the near-Earth region. This impulse launched a tailward propagating signal (rarefaction wave) that enhanced reconnection in the mid tail. Substorm intensification was correlated with the enhancement of the reconnection rate at the preexisting reconnection region located at 30 R_E. The importance of the electric field spike in correlating ionospheric and magnetospheric aspects of the substorm is emphasized.

Introduction

Substorms are the primary process by which energy extracted from the solar wind is impulsively released in the magnetosphere and ionosphere. The substorm paradigm [Kennel, 1995] was created on the basis of synthesis of spacecraft and ground observations spanning more than 35 years. From an observational viewpoint, the brightening of a preexisting auroral arc was the original definition of substorm onset [Akasofu, 1964], and it remains a central feature of substorms. The brightening occurs simultaneously with the sudden intensification of the local westward electrojet.

These ionospheric phenomena are closely correlated with activity in the near earth magnetotail. Observations indicate that most, if not all, substorms initiate near 6-10 R_E, a region connected to the arc that brightens at onset [e.g., Lopez et al., 1993]. Onset results in dipolarization of the near-Earth magnetic field and the creation of the substorm current wedge [McPherron et al., 1973]. In the near-Earth neutral line model, the formation of the current wedge is precipitated by a near-Earth reconnection region located at about 15 R_E to 20 R_E [e.g., Hesse and Birn, 1991; Baker et al., 1996].

It is generally accepted that reconnection occurs during substorms and that reconnection is the means by which energy stored in the lobes is released. The question is when, where, and how important is the formation of a reconnection region in the development of a substorm. It has been argued that reconnection begins in the growth phase [e.g., Baker and McPherron, 1990], at substorm onset [e.g., Hones, 1984], at some point during the expansion phase [e.g., Lopez, 1994], or at the onset of the recovery phase [e.g., Lui, 1991].

A critical issue in this question is the relationship between reconnection and phenomena such as auroral brightening and current sheet disruption [e.g., Lui et al., 1992] that mark expansion phase onset. Optical observations from spacecraft [e.g., Murphree et al 1991] and ground stations [e.g., Samson et al., 1992] have shown that substorm onset often occurs well away from the boundary between open and closed field lines, where reconnection of lobe field-lines would be occurring. And near-Earth activity, such as injections in geosynchronous orbit, can occur without evidence of the large-scale flows one expects from a significant unloading of lobe flux through reconnection [Lopez et al., 1994]. Yet it is equally clear that dayside merging and the loading of the tail lobes is a critical feature of the substorm growth phase, and that the release of the energy is an essential feature of the substorm sequence.

Our objective in this letter is to explore these issues using a global MHD simulation of an isolated substorm that occurred of March 9, 1995. In particular, we discuss the relationship between ionospheric phenomena and the global development of the substorm in the context of the simulation results. Our intent is to show that the MHD results are close enough to the observations that they likely reproduce much of the relevant physics and that the simulation can reconcile a near-Earth onset with the reconnection of lobe flux during the substorm.

The MHD Code

The simulations are based on the numerical solution of the ideal MHD equations that are used to model the solar wind and the outer (beyond 3 R_E) magnetosphere. These equations are numerically integrated as an initial value problem. We use a finite volume technique with Adams-Bashforth time marching and centered eighth-order spatial differencing. In addition non-linear numerical switches based on the Partial Donor Method [Hain, 1987] are used to maintain a total variance diminishing solution.

The numerical mesh is a computer generated, distorted spherical coordinate system with its axis of symmetry aligned with the solar wind flow. The outer boundaries are at x = 30 and -300 R_E and $y^2 + z^2 = 100\ R_E$. The inner boundary is at r = 3 R_E, where (x,y,z) are the solar magnetospheric coordinates (SM). The mesh is designed to afford maximal resolution near the bow magnetopause, the ionosphere and in the geomagnetic tail, with poorer resolution far from the earth in the solar wind and magnetosheath near the outer boundary. The total number of cells was 50(radial) x 24(polar) x 32(azimuthal). The radial resolution in the region of the magnetopause was about 1/3 R_E, with the resolution in the surface about 3 times larger.

The boundary conditions on the outside of the cylinder consisted of outflow conditions on the rear (tailward) boundary where the flow exited the grid supersonically. On all the other boundaries the conditions were specified by the Wind data for the period appropriately time shifted to the actual points on the boundary. The Wind magnetic field data showed B_X to be pretty close to a linear function of B_Y and B_Z. Most likely this means that the IMF direction of variation was not along the

Paper number 98GL00662.
0094-8534/98/98GL-00662$05.00

sun-Earth line, but tilted by roughly 45 degrees, mostly in the z-direction. We assumed this tilt in propagating the WIND data to the boundary. We also incorporated the Earth's dipole tilt, but at a constant value. All Wind data were interpolated to 1-minute resolution and transformed to the SM coordinate system corresponding to 0500 UT; this corresponds to a non-rotating dipole. The solar wind then entered the grid off axis by 16 degrees in the -z direction.

The inner boundary is matched to a line - tying ionosphere -- in the sense of Coroniti and Kennel [1973] -- with a spatially and temporally varying Hall and Pedersen conductivities. Field-aligned currents are mapped from the inner boundary to the ionosphere, where a convection electric field is computed. The electric field is then mapped to the inner boundary, where it is used to compute boundary conditions on the magnetic field and on the plasma momentum (see Fedder et al. [1995]).

Substorm activity on March 9, 1995

A particular substorm sequence on March 9, 1995 -- initially identified by Alan Rogers -- was studied using the MHD code. This period is particularly amenable to simulation because the IMF had been northward for an extended period of time, allowing the simulation to settle into a "ground state." Figure 1 shows the epsilon parameter, which estimates the energy input into the magnetosphere [Akasofu, 1981]. Epsilon was calculated using the solar wind data from Wind; a 7 RE merging line was assumed and the data have been lagged by the 54-minute propagation delay from Wind to Earth. At about 0330 UT, epsilon increased substantially due to a sudden southward rotation of solar wind magnetic field. A growth phase began at that time that was recorded by a number of ground stations [A. Rogers, personal communication, 1996].

Figure 2 shows an auroral electrojet index, CL, derived using only stations of the CANOPUS chain. Inspection of the available magnetometer data from CANOPUS and other sites indicates that the CANOPUS array was well situated to cover this substorm and that the onset took place close to the central meridian of the array. The onset of the substorm expansion phase began just before 0500 UT, as indicated by the drop in CL. There was a further intensification at 0514 UT, followed by a partial recovery, and a second expansion at 0552 UT.

Optical emission data from CANOPUS meridian scanning photometers are presented in the upper panels of Figure 3. The 6300 Å data from Rankin Inlet (RANK) serves as a proxy for the open-closed field line boundary [Samson et al, 1992; Blanchard et al., 1995], while the 5477 Å data provide information about auroral arc activity at Gillam (GILL) and Fort Smith (FSMI) two hours to the west. The data from RANK show that at about 0407 UT the polar cap boundary in that local time sector (the same meridian as GILL) began to move rapidly equatorward. Preexisting arcs at GILL and FSMI slowly moved equatorward during this growth phase.

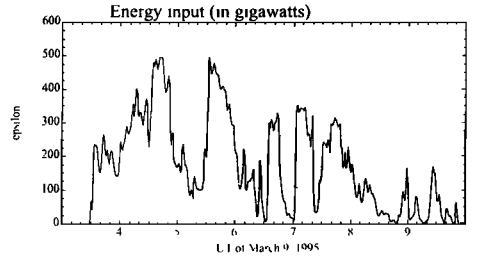

Figure 1 - Solar wind energy input (epsilon) for March 9, 1995 lagged by 54 minutes to reflect the propagation time from Wind to Earth. Note the sudden increases in energy input beginning at 0430 UT and 0530 UT, which are approximately 25 minutes before the two onsets in both the simulation and observations.

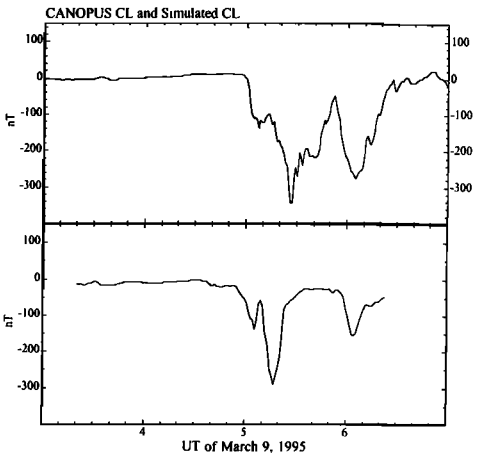

Figure 2 – Comparison of the CANOPUS CL index (upper panel) and the simulation CL (lower panel).

Just before 0500 UT, the 5477 Å data from GILL show a brightening of the auroral arc at about 67°. Immediately after the initial onset the polar cap boundary stayed essentially at the same latitude. Within a few minutes after 0500 UT, the polar cap boundary at RANK moved slightly poleward. At about 0515 UT, the aurora at GILL intensified and moved poleward. Shortly thereafter, at 0520 UT the polar cap boundary at RANK began to move rapidly poleward, suggesting that the polar cap was shrinking and the tail was unloading, as activity spread west into the FSMI sector. The poleward motion of the polar cap boundary stopped around 0533 UT, at which point the polar cap began to grow again. At about 0540 UT the boundary again began to move poleward (another unloading episode), until about 0555 UT, when it began to move equatorward again. This behavior of the aurora is very consistent with the magnetometer data and reflects a fairly commonplace evolution of a substorm.

Substorm Simulation

To compare the ionospheric response of the simulation to observations, the east-west component of the simulated Hall current in a box roughly defined by the extent of the CANOPUS array was translated into an H deflection by assuming that only the current maximum in the box contributed to the magnetic perturbation on the ground directly below the maximum. This provides a simulated CL, which is shown in lower panel of Fig. 2. The simulated CL reflects the major features of the substorm very well, even if the times do not exactly match the observations. There is an initial onset (0454 UT), an intensification (0508 UT), a recovery (0518 UT), and a second onset (0555 UT). Moreover, the magnitudes of CL and the simulated AL are in reasonable agreement.

The bottom panels of Figure 3 present the simulated polar cap flux (where the polar cap is defined as the open-closed field line boundary; the flux is integrated over both hemispheres), as well as the open-closed boundaries along the noon and midnight meridians. At 0330 UT, the polar cap began to grow, initially on the dayside, as a direct response to dayside merging. The midnight boundary did not move substantially equatorward until about 25 minutes later. If we consider that newly merged field lines are anchored at one end in the solar wind, a 25 minute lag suggests that the field line have been convected about 100 RE downstream (roughly the nominal tail length) before the growth of the polar cap hits midnight. It is important to note that RANK did not see rapid equatorward motion of the polar cap boundary until 0407 UT, which is a good indication that the 25 minute delay between noon and midnight in the simulation is a physically meaningful result.

The polar cap continued to add flux until about 0454 UT,

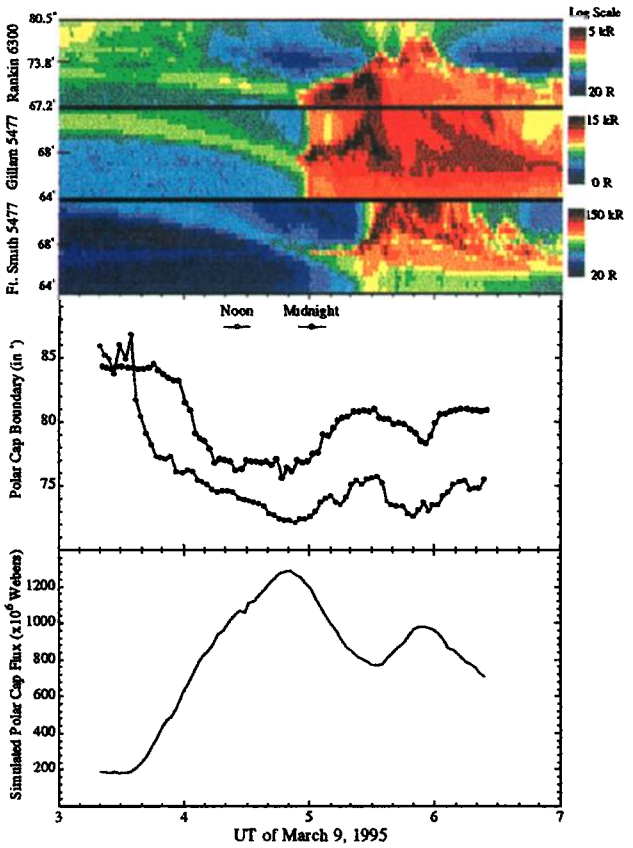

Figure 3 - Photometer data from the CANOPUS chain (top three panels), simulation open-closed boundaries (fourth panel), and simulation polar cap flux (bottom panel). The 25 minute propagation delay from the dayside to the nightside is apparent in the simulated polar cap boundaries.

when the polar cap began to shrink. The rate of flux decrease increased dramatically at 0508 UT and continued until 0536 UT, when the polar cap began to grow again. At 0554 UT the polar cap began to shrink. Each of these episodes of polar cap shrinkage corresponds to the unloading of stored energy in the magnetotail as represented by tail magnetic flux. Comparing to the data we see that the two main onsets were reproduced by the simulation, and that the behavior of the polar cap boundary in the simulation is remarkably similar to observations. In addition, comparison with Fig. 1 shows -- allowing for the 25 minute time lag from dayside to nightside -- both onsets correspond to large increases in the solar wind power input.

We now examine the behavior of the simulated magnetospheric electric field whose behavior is closely correlated with the ionospheric response. Figure 4 shows the magnitude of the electric field in the X-Z plane (displaced 2.5 RE to dusk to better track the onset). The top panel shows the magnetosphere prior to the growth phase. The middle panel is just after substorm onset (0457 UT). A reconnection region that formed about half an hour prior to onset is apparent at about 30 RE. The reconnection rate was slow so that the tail flux increased until just before onset. Another feature of note is the enhanced electric field in the inner region of the magnetotail. This electric field was stronger than and independent of the reconnection electric field further down the tail. Inspecting Fig. 1, we see that a sudden increase in solar wind energy began at 0430 UT. Given the 25 minute propagation delay discussed above, the effect of this pulse should have arrived at midnight at 0455 UT, as was the case.

Complete color animated sequences of both the electric field and the plasma density for this simulation are available at www.spp.astro.umd.edu under Global MHD Simulations. The animation shows that after the electric field impulse reached the center of the plasma sheet, it launched a tailward propagating signal that appears to be a rarefaction wave resulting from the inward convection surge associated with the

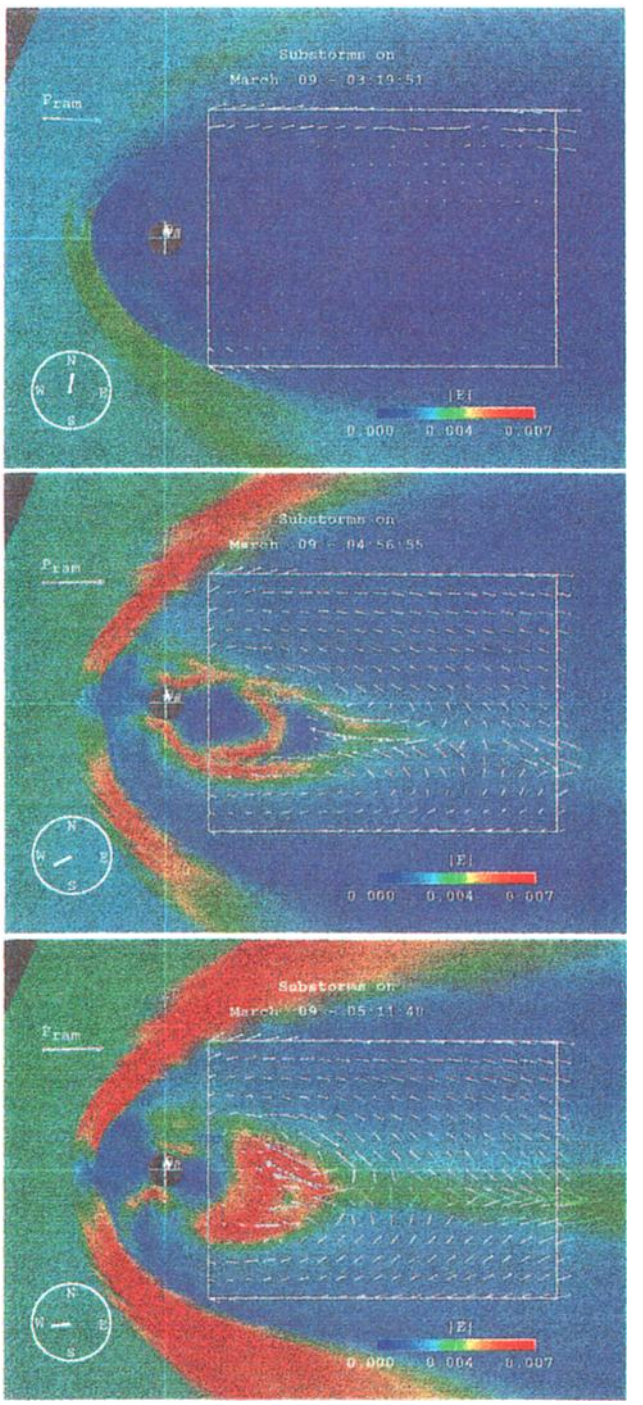

Figure 4 – The magnitude of electric field in the X-Z plane displaced 2.5 R_E duskward from the noon-midnight meridian. The white vector field in the tail region shows the magnitude and direction of the plasma flows. The P_{iam} and compass indicate the solar wind conditions at a point 15 R_E upstream. The first panel at 0320 shows a quiet tail configuration due to long duration of northward IMF. The second panel at 0457 UT, just after substorm onset, clearly shows and intensification of the electric field earthward of the mid tail reconnection region. The bottom panel at 0511 UT, just after the intensification, shows the enhancement of reconnection.

electric field spike. When this tailward propagating signal reached the preexisting reconnection region, the rate of reconnection increased markedly, a fact that can be easily seen by examining the flows in the bottom panel of Figure 4. After 0530 UT the rate of reconnection subsided. This, coupled with an increase in the newly merged flux at the dayside, resulted in a growth of the polar cap. The intensification of activity at 0555 UT in the simulation is also of considerable interest. In contrast to the 0454 UT activity, there was no electric field penetration in the near-Earth region, even though at 0530 UT there was another burst of energy supplied by the solar wind. This energy apparently went directly into the reconnection region, triggering a second episode of unloading.

Summary and Conclusions

The global MHD simulation reproduced the general features of the March 9, 1995 substorm to a surprising degree. There are two main onsets, as seen in the CANOPUS CL. The 0552 UT onset in the CANOPUS data occurred at high latitudes, near the open-closed field line boundary. In the simulation it also occurred at that boundary, with no near-Earth penetration of electric field as in the initial onset. The general evolution of the polar cap flux in the simulation appears to agree qualitatively with the variation of the open-closed field line boundary at Rankin. There are also differences between the simulation and the observations, among which being that prior to onset there is no observational evidence from CANOPUS that polar cap had begun to shrink. The onset, in fact, occurred at fairly low latitudes, well away from the open-closed field line boundary. It was only several minutes later that activity reached the open-closed field line boundary and the boundary moved poleward.

The primary energy release in the simulations appears to be through reconnection of tail lobe flux. This release appears to begin before the onset as viewed on the ground. However, a clear onset is associated with activity in the near-Earth region, far away from the open-closed boundary. Why does this occur?

A partial answer is related to the imbalance between the reconnection site and the site of Poynting flux deposition. A simple vacuum superposition of a dipole field confined to the magnetosphere with a 10-20% addition of the IMF shows that the field null in the tail will occur in the neighborhood of 20-30 RE. By contrast, the Poynting flux from the solar wind concentrates in the near-Earth region as pointed out by Papadopoulos et al. [1993]. The simulations confirm this result. The convergence of the Poynting flux is primarily in the near-Earth region. The energy (and stresses) are delivered to a place far removed from the one where they can be processed -- the reconnection site. This leads to a stretching of the near-Earth tail during growth phase. At onset, this stress is relieved leading to creation of the substorm current wedge at much lower latitude than the reconnection site. However, the effects of the near-Earth disruption are communicated to the reconnection site, where they lead to enhanced reconnection and release of the tail lobe magnetic energy. This process also leads to a reconfiguration of the tail, such that electromagnetic energy can flow more directly into the reconnection site. In terms of Poynting flux, the optics of the magnetosphere have changed to allow direct driving of tail reconnection. Note that the simulated 0555 UT substorm onset does not have a near-Earth onset; the magnetosphere remains in the late substorm configuration.

The onset of the substorm is clearly related to the disruption of this stressed configuration in the near-Earth region. What triggers the onset is still not clear. In principle all the necessary information to detail the physical mechanism of the substorm triggering is available in the simulation. It is certainly striking that the arrival of a surge in Poynting flux in the near-Earth region, approximately 25 minutes after the increase in epsilon seen in Figure 1, more or less coincides with the onset. However, we have not yet designed the diagnostics necessary to test whether the tail response is simply driven, pushed over an instability threshold, or spontaneously unstable. If unstable, what is the instability? We are working on these issues, and this letter is in way of a progress report, not a final answer.

Acknowledgments: The authors would like to thank Alan Rodgers for providing data for this event and for stimulating discussions. We would also like to thank John Sampson for generously provide CANOPUS magnetometer and optical data. This work was supported by NASA grants NAG-51101, NAG-56256, NAG-54662, and NAGW-3222, and by NSF grant ATM-9527055.

References

Akasofu, S.-I., The development of the auroral Substorm, *Planet. Space Sci., 12*, 273-282, 1964.

Akasofu, S.-I., Energy coupling between the solar wind and the magnetosphere, *Space Sci. Rev., 28*, 121, 1981.

Baker, D. N., and R. L. McPherron, Extreme energetic particle decreases near geostationary orbit: A manifestation of current diversion within the inner plasma sheet, *J. Geophys. Res., 95*, 6591-6599, 1990.

Baker, D. N., T. I Pulkkinen, V. Angelopoulos, W. Baumjohann, and R. L. McPherron, Neutral line model of substorms: Past results and present view, *J. Geophys. Res., 101*, 12975-13010, 1996.

Blanchard, G. T., L. R. Lyons, J. C. Samson, F. J. Rich, Locating the polar cap boundary from observations of 6300 Å auroral emission, *J. Geophys. Res., 100*, 7855-7862, 1995.

Coroniti, F. V. and C. F. Kennel, Can the ionosphere regulate magnetospheric convection?, *J. Geophys. Res.*, 78, 2837, 1973.

Fedder, J. A., S. P. Slinker, J. G. Lyon, and R. D. Elphinstone, Global numerical simulation of the growth phase and the expansion onset for substorm observed by Viking, *J. Geophys. Res.*, 100, 19083, 1995.

Hain K., The partial donor method, *J. Comp. Phys.*, 73, 131, 1981.

Hesse, M. and J. Birn, On dipolarization and its relationship to the substorm current wedge, *J. Geophys. Res., 96*, 19417-19426, 1991.

Hones, E. W., Jr., Plasma sheet behavior during substorms, in *Magnetic Reconnection in Space and Laboratory Plasmas*, edited by E. W. Hones, Jr., 178-184, AGU, Washington, D. C., 1984.

Kennel C.F. Convection and Substorms, Oxford University Press, 1995.

Lopez, R. E., H. E. J. Koskinen, T. I. Pulkkinen, T. Bösinger, T. A. Potemra, and R. W. McEntire, Simultaneous observation of the poleward expansion of substorm electrojet activity and the tailward expansion of current sheet disruption in the near-Earth magnetotail, *J. Geophys. Res., 98*, 9285-9295, 1993

Lopez, R. E., C. C. Goodrich, G. D. Reeves, R. D. Belian, and A. Taktakishvili, Mid-tail plasma flows and the relationship to near-Earth substorm activity: A case study, *J. Geophys. Res., 99*, 23561-23569, 1994.

Lopez, R. E., On the role of reconnection during substorms, *Proc. International Conference on Substorms-2*, 175-182, 1994

Lui, A. T. Y., A synthesis of magnetospheric substorm models, *J. Geophys. Res., 96*, 1849, 1991.

Lui, A. T. Y., R. E. Lopez, B. J. Anderson, K. Takahashi, L. J. Zanetti, R. W. McEntire, T. A. Potemra, D. M. Klumpar, E. M. Greene, and R. Strangeway, Current disruptions in the near-Earth neutral sheet region, *J. Geophys. Res., 97*, 1461-1480, 1992.

McPherron, R. L., C. T. Russell, and M. P. Aubry, Satellite studies of magnetospheric substorms on August 15, 1968. 9. Phenomenological model for substorms, *J. Geophys. Res., 78*, 3131-3149, 1973.

Murphree , J. S., R. D. Elphinstone, L. L. Cogger, and D. Hearn, Viking opitcal substorm signatures, in *Magnetospheric Substorms, Geophys. Monogr. Ser.*, vol. 64, edited by T. Iijima, T. A. Potemra, and J. R. Kan, pp. 241-255, AGU, Washington, D.C., 1991.

Papadopoulos, D., S. Sharma and J. Valdivia, Is the Magnetosphere a Lens for MHD Waves?, *Geophysical Research Letters, 20*, 2809-2812, 1993.

Samson, J. C., L. R. Lyons, P. T. Newell, F. Creutzberg, B. Xu, Proton aurora and substorm intensifications, *Geophys. Res. Lett., 19*, 399-402, 1992.

C. C. Goodrich and R. E. Lopez, Department of Astronomy, K Papadopoulos, and M Wiltberger, Department of Physics, University of Maryland College Park, MD 20742. (e-mail Internet ccg@avl.umd.edu, lopez@astro.umd.edu, kp@astro.umd.edu,)

J.Lyon, Department of Physics, Dartmouth College, Hannover, NH, 03755 (e-mail Internet lyon@tinman.darmouth.edu)

(Received October 24, 1997; revised January 15, 1998; accepted February 3, 1998.)